DOE/PC/79930--T9

MAY 04 1992

DOE/PC/79930--T9

DE92 013608

PYROLYSIS AND GASIFICATION OF COAL AT HIGH TEMPERATURES

Grant Number DE-FG22-87PC79930

QUARTERLY PROGRESS REPORT

(Quarter #5 : 9/15/1988 to 12/15/88)

PRINCIPAL INVESTIGATOR: Prof. Kyriacos Zygourakis
Department of Chemical Engineering
Rice University
Houston, Texas 77251-1892
Tel. (713) 527-8101 Ext. 3509.

PROJECT MANAGER: Dr. James Longanbach
Morgantown Energy Technology Center
PO Box 880
Collins Ferry Road
Morgantown, West Virginia 26505.

GRANT PERIOD: 9/15/1987 to 9/14/1990

US/DOE Patent Clearance is **not** required
prior to the publication of this document

SHORT DESCRIPTION OF TASKS

(A) Effects of Pyrolysis Conditions on Macropore Structure

Coals of different ranks will be pyrolyzed in a microscope hot-stage reactor using inert and reacting atmospheres. The macropore structure of the produced chars will be characterized using video microscopy and digital image processing techniques to obtain pore size distributions. Comparative studies will quantify the effect of pyrolysis conditions (heating rates, final heat treatment temperatures, particle size and inert or reacting atmosphere) on the pore structure of the devolatilized chars.

(B) Gasification Under Strong Intraparticle Diffusional Limitations

The devolatilized chars will be gasified in the regime of strong intraparticle diffusional limitations using O_2/N_2 and $O_2/H_2O/N_2$ 2 mixtures. Constant temperature and programmed-temperature experiments in a TGA will be used for these studies. Additional gasification experiments performed in the hot-stage reactor will be videotaped and selected images will be analyzed to obtain quantitative data on particle shrinkage and fragmentation.

(C) Mathematical Modeling and Model Validation

Discrete mathematical models will be developed and validated using the experimental gasification data. Structural properties of the unreacted chars will be used to generate computational grids simulating the pore structure of the solid. Simulations will then provide the evolution of observed reaction rates with conversion. The size distribution of particle fragments obtained as the reaction front moves through the particle will also be obtained. Proper statistical averaging of the results from these simulations will yield the expected behavior for each char. Comparisons of experimental data and theoretical predictions will identify the fundamental phenomena that must be included in a mathematical description of the process, thus leading to the development of accurate models for the gasification of coal particles.

1. SUMMARY

A new procedure was developed to smooth the binary images used for computing macropores structural properties. This procedure will minimize the errors introduced by image noise and pixelization effects and will also improve the accuracy of model predictions. The furnace of our thermogravimetric system has been redesigned and we can now achieve heating rates as high as 1200-1500 °C/min (or 20-25 °C/s). Such heating rates are almost an order of magnitude larger than those attainable with the manufacturer's furnace. The new furnace design will allow us to perform pyrolysis experiments at fairly high heating rates in the thermogravimetric reactor, thus facilitating the collection and analysis of data. We have also computerized the gas feed system with its mass flow controllers whose operation can now be programmed, controlled and monitored via the data acquisition and control microcomputer. The new setup will allow us to quickly and reproducibly switch gases during an experiment minimizing the transients during constant temperature gasification experiments. Finally, the simulation codes were modified so that they can model reaction in the regime where diffusional limitations in the macropores are negligible. The predicted reactivity behavior of our devolatilized chars is compared and analyzed.

2. TECHNICAL AND SCIENTIFIC RESULTS

(A) Effects of Pyrolysis Heating Rate on Macropore Structure of Chars

The porosity and macropore surface area measurements presented in earlier reports were obtained from digitized images of char particle cross-sections. These measurements involve: (a) acquisition of grey-level (black & white) images with 640x480 pixel resolution; (b) segmentation of the B&W images to to obtain binary images; and (c) processing of the binary images to identify the macropores and measure their statistics. The pores identified on the original binary images have very jagged edges due to pixelization errors introduced during the

acquisition and segmentation steps. Such pixelization errors are evident, for example, in the original 640x480 pixel binary image shown in Fig. 1A.

We have developed a new procedure for smoothing the pore (and particle) boundaries in order to eliminate possible artifacts introduced by the pixelization errors. Each 640x480 image is converted to an artificial B&W image with only two grey levels (black and white). A filter with a 3x3 kernel is then applied to the BW image resulting in a "blurring" of the sharp boundaries. The filtered image is then segmented and magnified by a factor of 4 to obtain a binary image with smooth boundaries. Fig. 1B also shows the smoothed 2560x1920 image obtained by applying this procedure on the original binary image. The pixelization that led to boundary jaggedness has been eliminated in the smoothed image. Also, several small pores consisting of one or two pixels have been filtered out. This is another desirable result of the smoothing operation, since pores with only a few pixels may be due to noise in the original image. Finally, one should note here that one large internal macropore in the original image of Fig. 2A opened to the exterior; the smoothing operation broke the wall of this pore at a point where it was only one pixel wide.

The smoothing procedure will thus change the macropore structural properties. A comparison of the average properties for the images of Fig. 1 is given in Table I. below.

TABLE I

Comparison of Average Macropore Properties for Original and Smoothed Binary Images of Figure 1

	Number of Macropore Profiles	Total Area of Macropore Profiles (μm^2)	Average Area of Macropores (μm^2)
Original	95	49,441	520.7
Smoothed	80	47,143	588.4

Fig. 2 also shows that the perimeters of the macropore profiles decrease as a result of the smoothing operation. Thus, one would expect to compute slightly smaller values of macropore surface areas. A systematic investigation of the effects of smoothing is under way. The computations are complicated by the fact that the binary images are now 16 times larger. This procedure, however, will produce results that should be free of noise and pixelization errors.

(B) Gasification Under Strong Intraparticle Diffusional Limitations

The development work for the thermogravimetric reactor continued. A new furnace design allows us now to achieve sustained linear heating rates of at least 600 °C/min (or 10 °C/s) for a final temperature between 900 and 1000 °C. If a final heating temperature around 500 °C is desired, then faster heating rates in the range of 1200-1500 °C/min (or 20-25 °C/s) can be achieved. These heating rates are almost an order of magnitude larger than the rates attainable with the furnace provided by the manufacturer of the instrument. We are still experiencing some problems with long term operation of the furnace at high temperatures and in an oxidizing atmosphere. These problems will be overcome by changing the wire used for furnace winding to a Kanthal alloy that is much more resistant to oxygen at temperatures above 800 °C.

The new furnace opens some new possibilities for our pyrolysis/gasification experiments. For example, pyrolysis experiments at fairly high heating rates can be performed in the thermogravimetric reactor. We should note here that our earlier pyrolysis experiments in the captive sample (heated grid) microreactor showed that the macropore structure of the produced chars exhibited the most drastic changes for heating rates between 0.1 and 10 °C/s. Chars produced at 10 °C/s already had the characteristic cellular internal structure with thin walled cavities and the specific macropore surface area appeared to reach a maximum at that heating rate. It thus seems possible now to carry out the bulk of pyrolysis

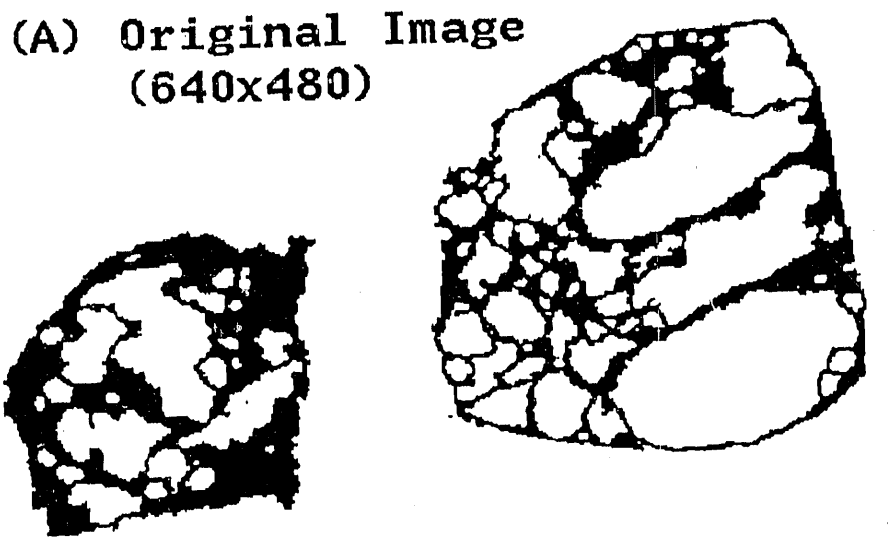

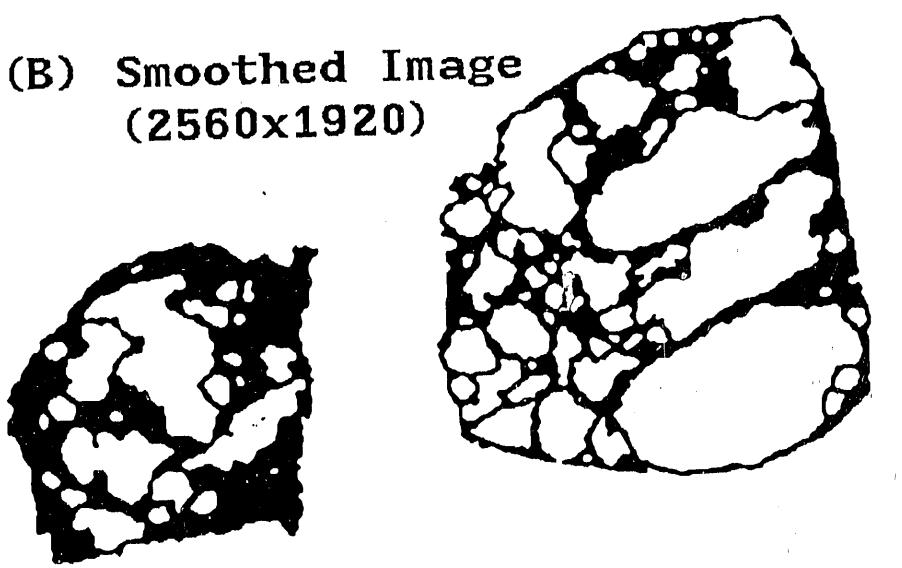

Figure 1: Original (A) and smoothed (B) images for two char particle cross-sections.

(A) Original Image (640x480)

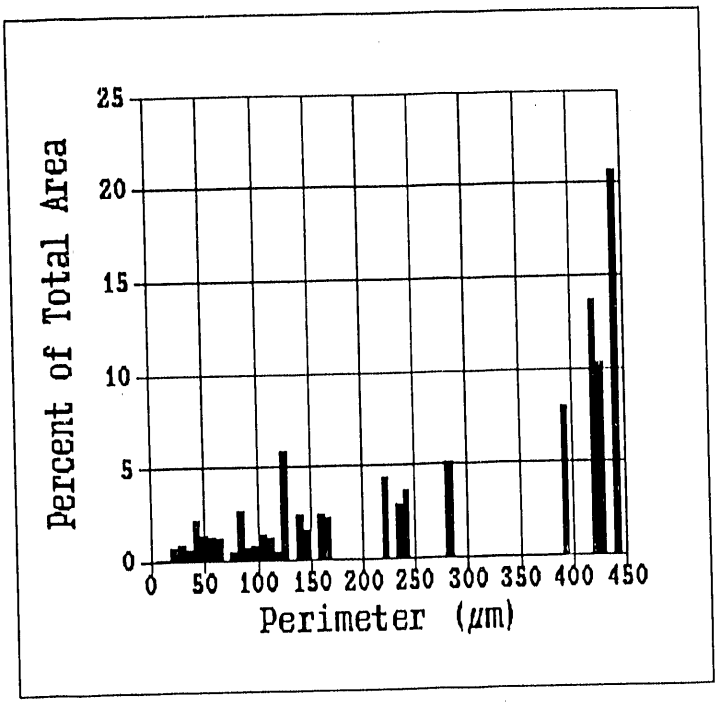

(B) Smoothed Image (2560x1920)

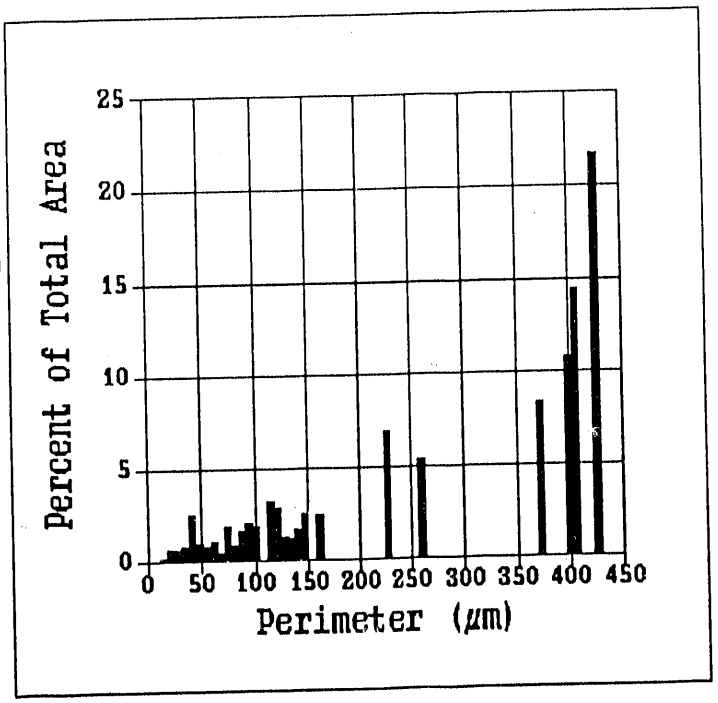

Figure 2: Histogram showing the size distribution of the perimeters of the macropore profiles calculated from an original image (A) and its smoothed counterpart (B).

and gasification experiments in one reactor system, thus simplifying the acquisition and interpretation of data.

Another major feature of our reactor system involves the incorporation of the gas feed system with its mass flow controllers into the computer control program. Mass flow controller operation can be programmed, controlled and monitored by the computer with three voltage signals for each unit. One signal (ON/OFF) switches each mass flow controller from LOCAL (dedicated readout unit has control) to REMOTE operation (computer has control). A second 0-5V signal provides the setpoint (flow rate) for the mass flow controller. The computer can also monitor the flow rate via a third 0-5V signal that is fed from the readout unit to the microcomputer. This setup will allow us to to quickly and reproducibly switch gases (e.g. from an inert to a reacting atmosphere) at any desired point in the temperature program. Computer control will minimize transients during constant temperature gasification experiments. During such experiments the coal sample will be heated to the final temperature in an inert atmosphere and and the gaseous reactant will be introduced when the reactor temperature has stabilized.

Fig. 3 shows a schematic of our thermogravimetric reactor setup with the computer analog/digital interfaces, the computerized gas feed system, the PDP-11/23+ microcomputer dedicated to data acquisition and control tasks and the MicroVAX computer where all the data are transferred for processing and analysis.

(C) Mathematical Modeling of Char Gasification

Our earlier numerical simulation studies had assumed that only the macropores directly accessible to reactants from the irregular particle exterior participate in the reaction. Internal macropores are not initially accessible to the gaseous reactants. When the reaction front "opens" these interior pores, however, their surface area becomes available for reaction. This reaction regime

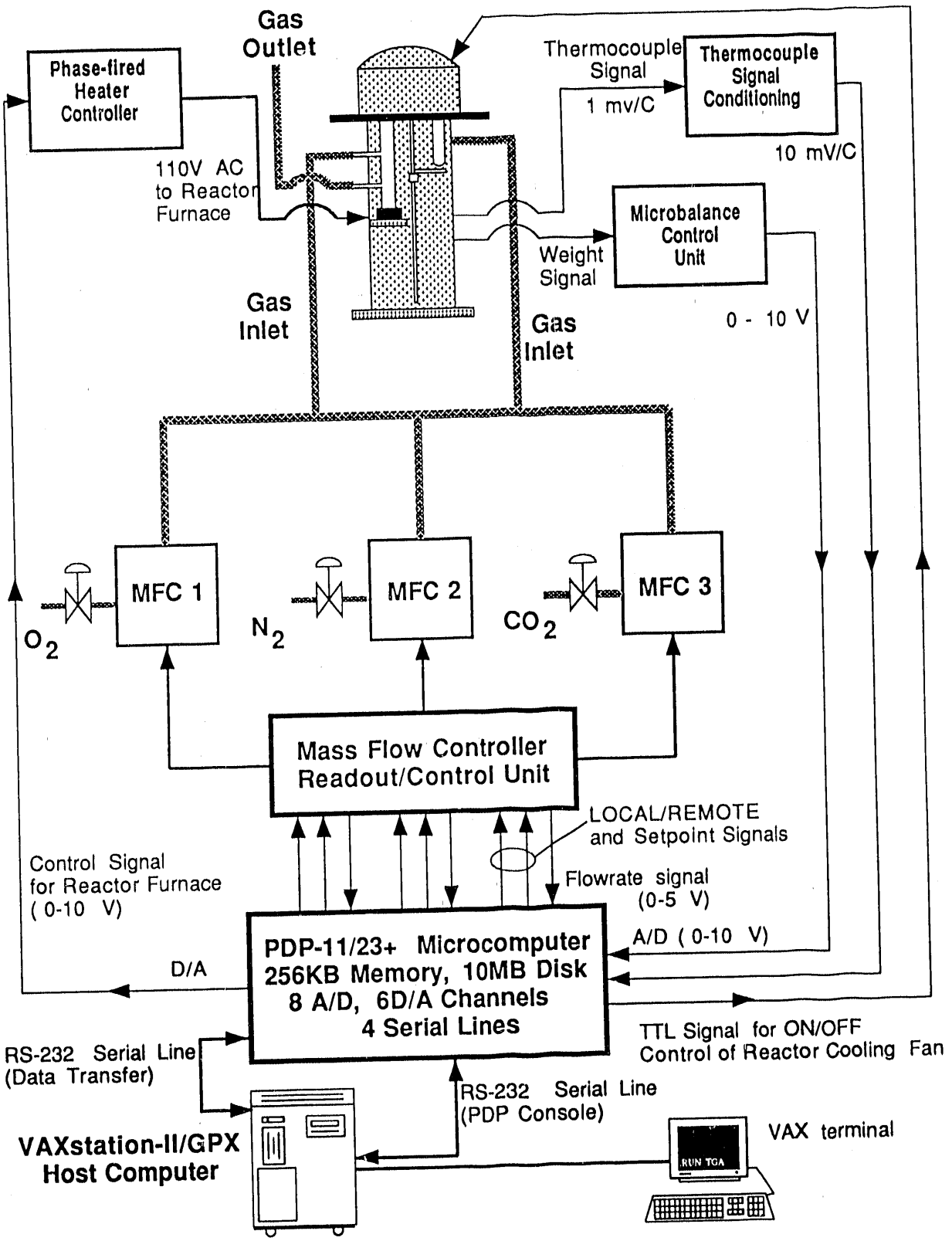

Figure 3: Schematic of the thermogravimetric reactor showing the computer interfaces, the computerized gas feed system, the control microcomputer and the host computer.

will be hereafter referred to as ***Regime B***. The rules describing reaction in this regime were implemented by allowing each cell of the computational grid to exist in one of three possible states (see Fig. 4A): it could be a solid reactant cell (black), a cell occupied by gaseous reactants or "open pore cell" (white) or a cell belonging to a "closed macropore" (grey). The initial cellular array was updated according to the following rules: ***(1)*** A solid reactant (black) cell may "react" (changing its state to white), if its immediate neighborhood contains one or more gaseous reactant (white) cells; ***(2)*** A solid reactant (black) cell will not change its state, if it is surrounded only by solid (black) or "closed pore" (grey) cells; ***(3)*** If "closed pore" (grey) cells get exposed to gaseous reactant (white) cells, their state may change to gaseous reactant (white). Figs. 4B and 4C show the configuration of the cellular array of Fig 4A at two different iteration steps and Fig. 4D again shows the evolution of the predicted reaction rate. In general, gaseous reactant cells "consume" solid or closed pore cells at different rates. These rates can be appropriately adjusted to account for different degrees of diffusional limitations in the macropores opening up for reaction.

Since the macropores observed at least with the Illinois #6 chars are very large, one might observe that even at relatively high temperatures diffusional limitations in the macropores may be negligible. In this case, the entire surface area associated with the macropores is available for reaction. This reaction regime will be hereafter referred to as ***Regime A***. In order to model reaction in this regime, each cell of our computational grid can exist in one of two possible states: it can represent a small volume element of either solid reactant or pore void. An initial computational grid for this regime is shown in Fig. 5A. The evolution of the pore structure is modeled by updating the initial cellular array at equally spaced time instants $t^1, t^2, \ldots, t^r, t^{r+1}, \ldots$ as follows: *If at time t^r a solid reactant (black) cell is adjacent to one or more gaseous reactant (white) cells, then this solid cell may be changed to a pore void cell or* ***reacted*** at the next time level $t^{r+1} = t^r + \Delta t$. The solid cells are reacted

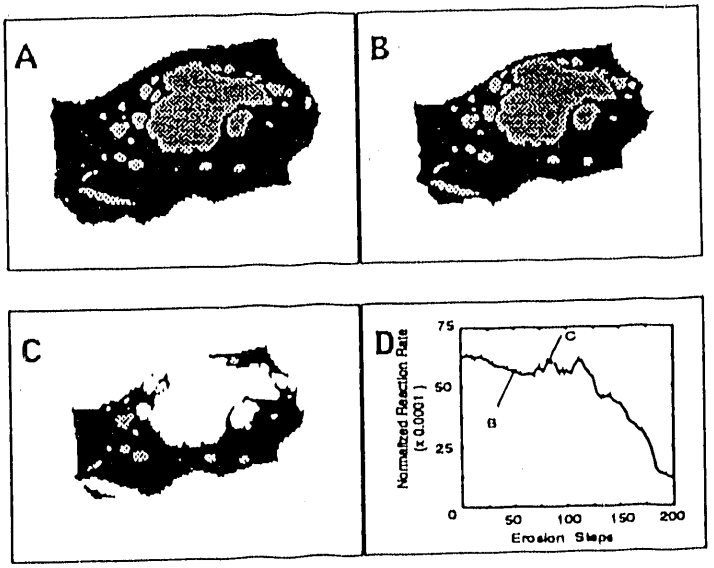

Figure 4: Binary images showing the computational grids at three conversion levels (A: initial; B: 30.9%; C: 49.1%) and the temporal evolution of reactivity for a simulation in Regime B.

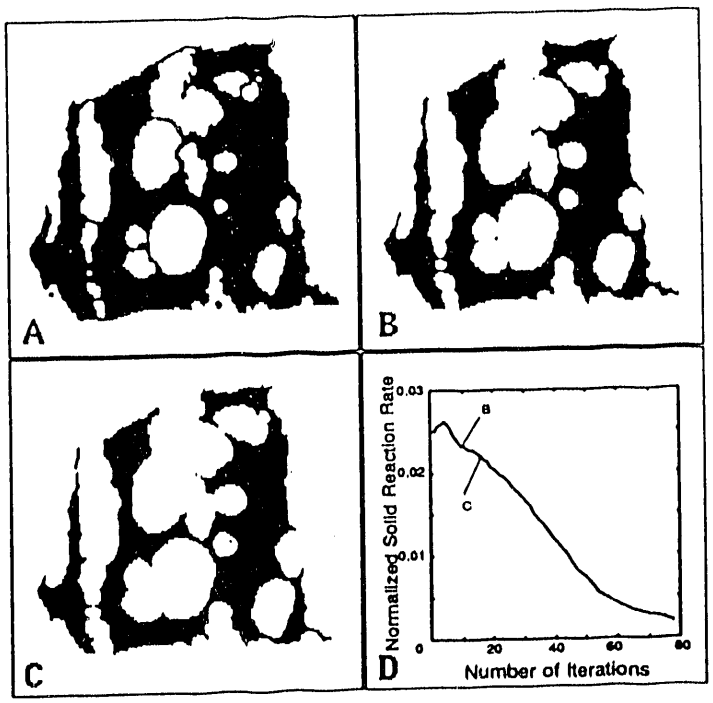

Figure 5: Binary images showing the computational grids at three conversion levels (A: initial; B: 24.9%; C: 38.4%) and the temporal evolution of reactivity for a simulation in Regime A.

according to a probabilistic algorithm that guarantees isotropic consumption of the solid reactant. This algorithm erodes a single layer of pixels from the entire surface area exposed to gaseous reactants during each iteration step Δt. Figs. 5B and 5C show the computational grid of Fig. 5A after 10 and 16 iteration steps that correspond to solid conversions of 24.9% and 38.4%. Fig. 5D shows the temporal evolution of the predicted reaction rate as a function of the number of iterations.

Under some fairly general assumptions, two-dimensional simulations can provide unbiased estimates of the reactivity of three-dimensional structures if the rection takes place in regime A. Our simulations are performed on two-dimensional cellular arrays that are discrete approximations of cross-sections of actual char particles. At each iteration step, heterogeneous reactions occur at the boundaries (perimeter) of the two-dimensional pore profiles (see Figs. 4 and 5). Results from ***two-dimensional simulations***, however, can be used to obtain accurate ***estimates*** of reaction rates occurring on our ***three-dimensional structures***. If we assume that the cross-sections used for our simulations form a "random plane section" through our population of char particles, unbiased estimators of the macroporosity ε and of the macropore surface density S_v (in (cm^2 pore surface)/(cm^3 particle)) are given (Weibel, 1980) by

$$\varepsilon = \frac{A_a}{A_c} \qquad S_v = \frac{1}{4\pi}\,\frac{B_a}{A_c} \tag{1}$$

where A_a is the total area of pore profiles, B_a is the total pore profile boundary length and A_c is the total area of particle cross-sections. Note that S_v can be estimated from two-dimensional sections ***without any restricting assumptions concerning the geometrical shape of the pores*** (DeHoff, 1983). The three primary quantities A_a, A_c and B_a can be easily obtained from the particle cross-sections via image processing techniques, and the total specific macropore surface area S_t (expressed in m^2 per kg of solid) can be easily computed as

$$S_t = \frac{S_v}{(1-\varepsilon)\ \rho_s} \tag{2}$$

where ρ_s is the density of the solid reactant. When reaction takes place in Regime A, there are no diffusional limitations in the macropores and the entire macropore surface area reacts at the same rate ($S_g = S_t$). If we assume that the evolving cross-sections continue to constitute "random sections" for our char particle population, the discrete simulations provide accurate ***estimates*** of the changing surface area of the ***three-dimensional macropores*** and, consequently, of the temporal evolution of reaction rates in Regime A. Although these arguments do not hold in the general case of reaction in Regime B (where the internal macropores are assumed to be initially "closed"), approximate estimates of reaction rates can be obtained if we assume that the internal pores for any cross-section do not become available for reaction due to burn-through occurring at planes above or below the studied one. Although this assumption can be easily relaxed in our discrete models, such an extension of the models would require information about the connectivity of the three-dimensional macropores. Such structural information is not currently available.

Simulations modeling reaction in regime A were performed on the same binary images of coal particles used in our earlier studies. However, the binary images were now smoothed and magnified according to the procedure described in Section 2A. This smoothing improved significantly the accuracy of our simulations, especially for the char samples exhibiting thin-walled vesicles. These thin walls are consumed in one or two iterations when the images are not magnified. For most of the simulations, each 640x480 image was magnified by a factor of 4. Several runs were also carried out by magnifying the original images by a factor of 8 and smoothing them. Fig. 6 shows that the results obtained from simulations with 5120x3840 images differ very little from the results obtained from simulations with 2560x1920 images. As before, 48 runs were performed with different particle cross-sections for each char sample and the results were averaged.

When there are no diffusional limitations in the macropores, the entire macropore surface area reacts at the same rate. Fig. 7 presents the reactivity patterns predicted for 4 chars produced from an Illinois #6 coal at different

pyrolysis heating rates. The model predictions reflect the wide differences in the pore structure of these chars (see our earlier reports and Zygourakis, 1988). All chars exhibit an initial increase in reactivity caused by macropore growth. Since the chars produced at high heating rates (10 and 1000 °C/s) have almost exclusively large thin-walled cavities, the predicted rates drop dramatically when the thin walls separating the macropores are consumed. The rate vs. conversion patterns exhibit a small maximum that is shifted towards higher conversion levels for the chars produced at high heating rates. Fig. 8 shows the predicted reactivity behavior for three chars produced from different size fractions of Illinois #6 coal particles at a pyrolysis heating rate of 10 °C/s. Small coal particle sizes lead to chars with larger macropore surface areas and, hence, with higher reactivity. These high reaction rates fall rapidly, however, and the maximum in the rate vs. conversion pattern shifts towards lower conversions. Fig. 9 shows the predicted reactivity behavior for two chars produced from a lignite coal at 0.1 and 1000 °C/s. Small differences in char reactivity can be seen from these graphs, an observation consistent with the pyrolysis mechanism and the pore structure of these chars.

REFERENCES

DeHoff, R.T., *J. Microscopy*, ***131***, 259 (1983).

Weibel, E.R., *Stereological Methods*, vol. *2*, Academic Press (1980).

Zygourakis, K., *ACS Div. Fuel Chem. Preprints*, ***33(4)***, 951 (1988).

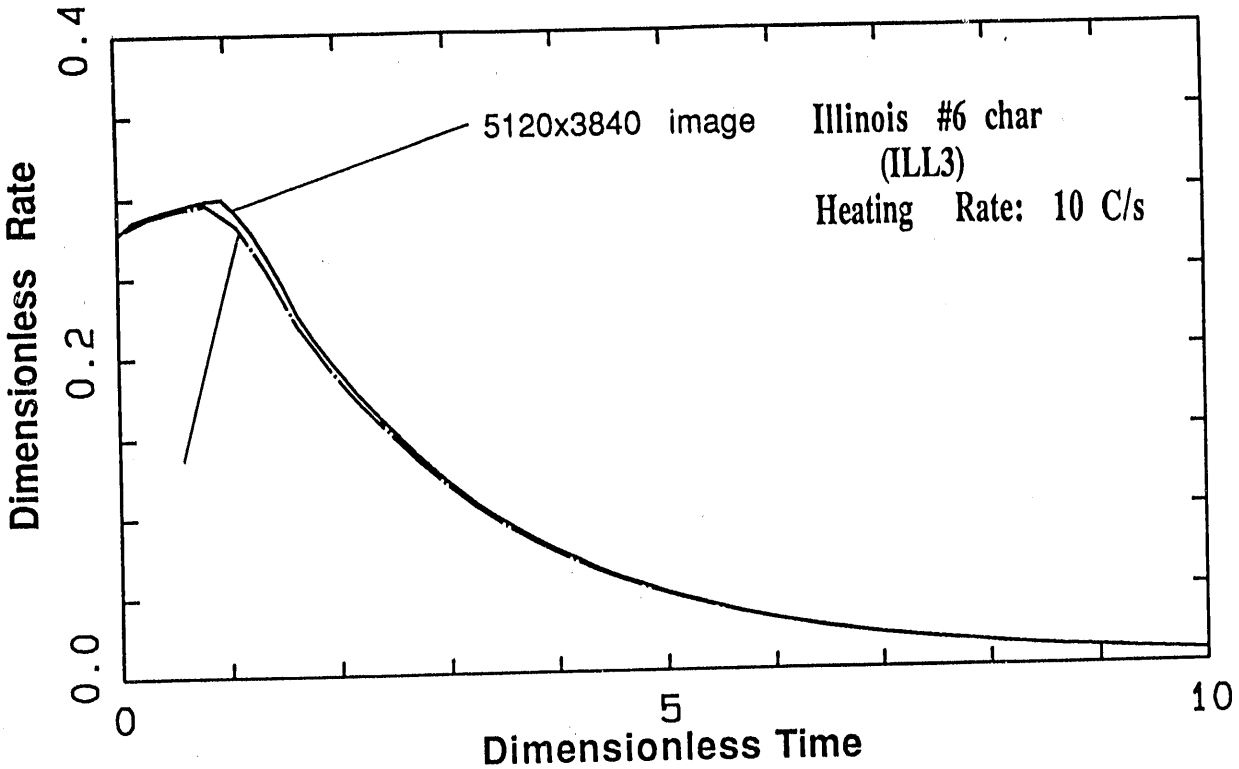

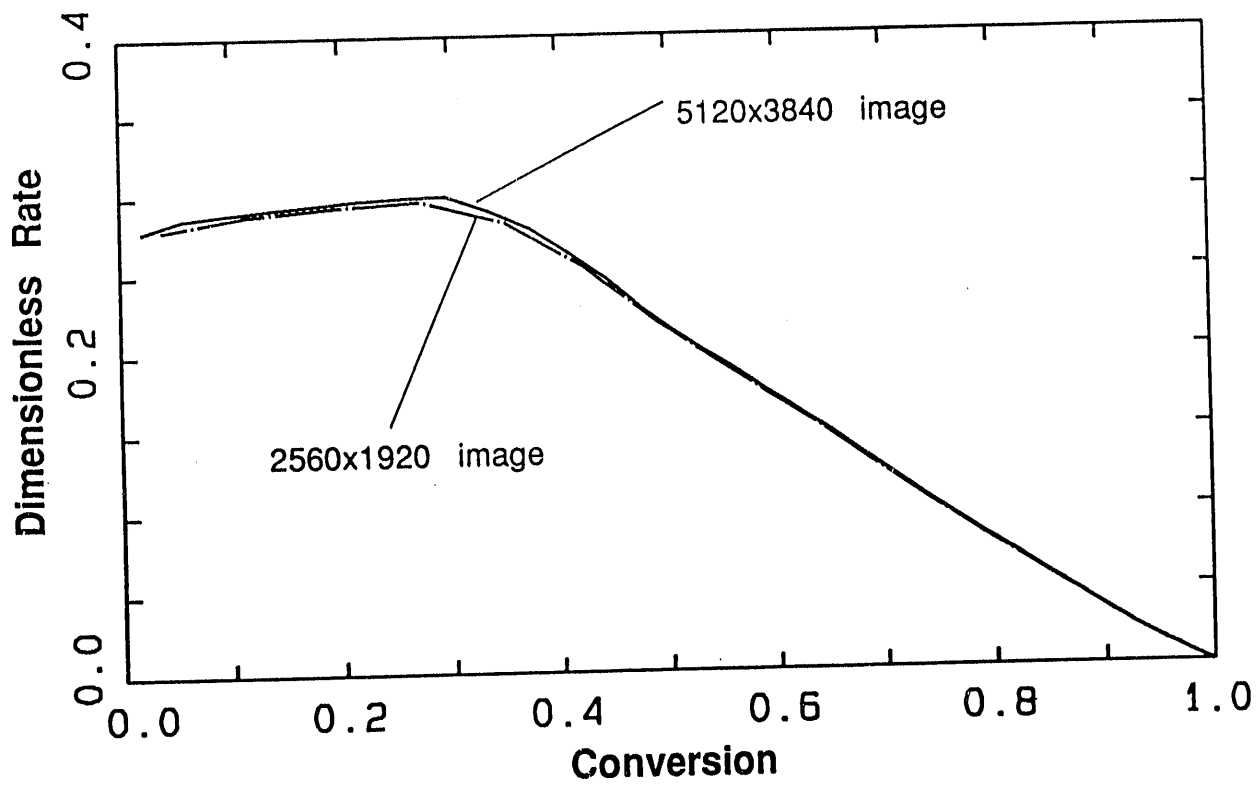

Figure 6: Reactivity patterns predicted for an Illinois #6 char in Regime A using 2560x1920 and 5120x3840 pixel images for the simulation runs. Each curve is the average computed from 48 runs with different particle cross-sections.

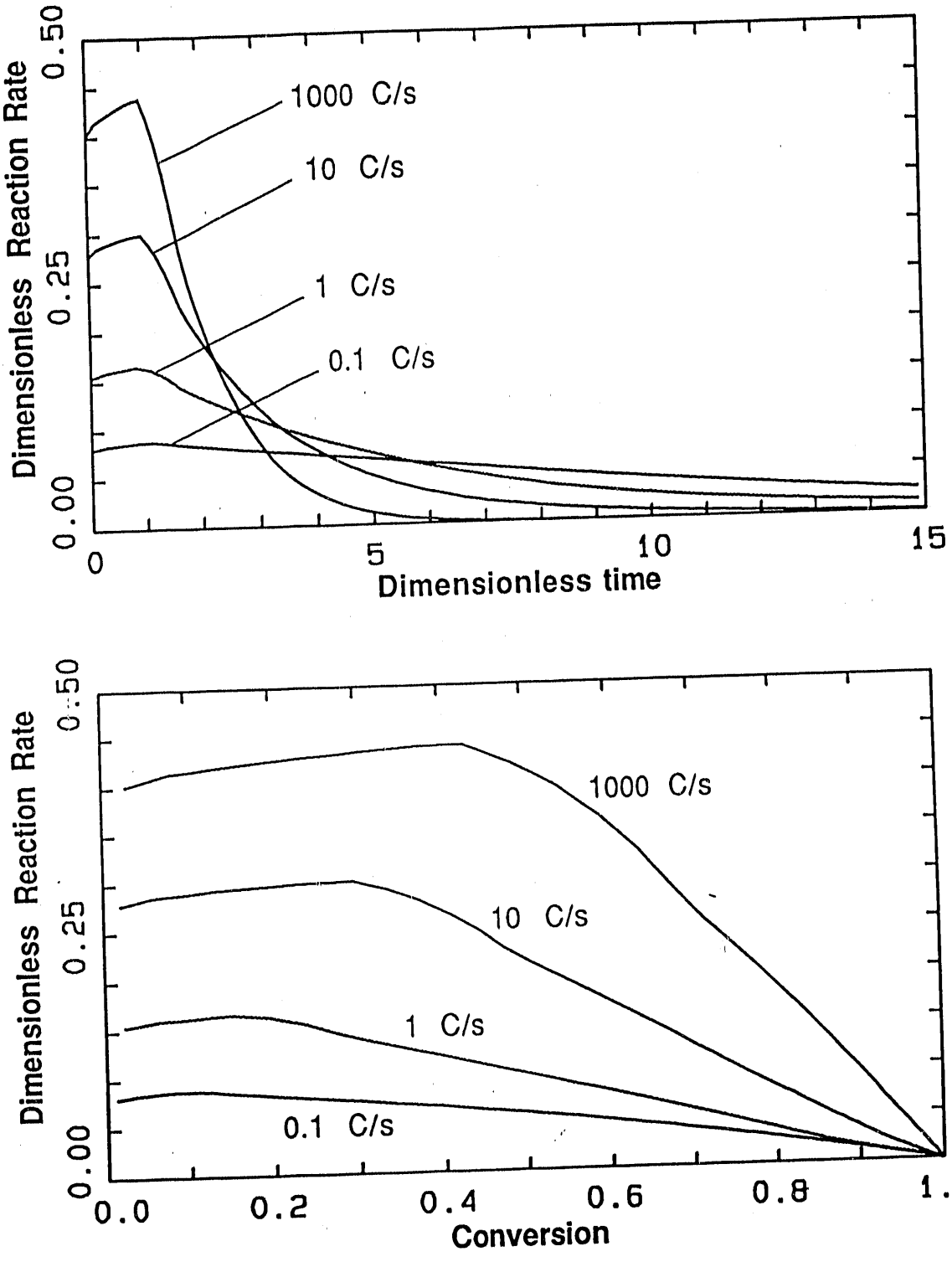

Figure 7: Reactivity patterns predicted for reaction in Regime A of four Illinois #6 chars produced at different pyrolysis heating rates (Coal particle size: 50-60 mesh). Each curve is the average computed from 48 runs with different particle cross-sections.

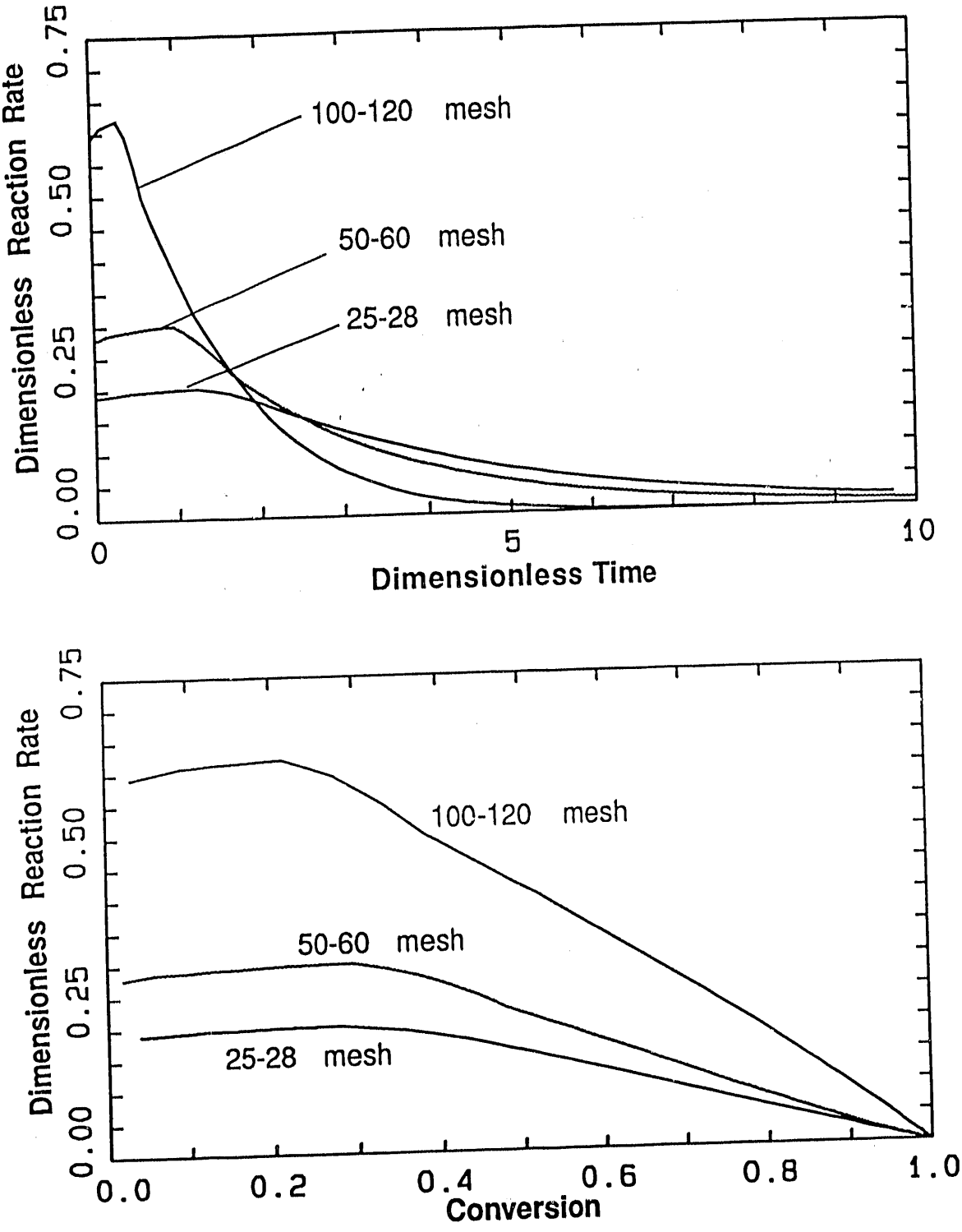

Figure 8: Reactivity patterns predicted for reaction in Regime A of three Illinois #6 chars produced from different coal particle size fractions (Pyrolysis heating rate: 10 °C/s). Each curve is the average computed from 48 runs with different particle cross-sections.

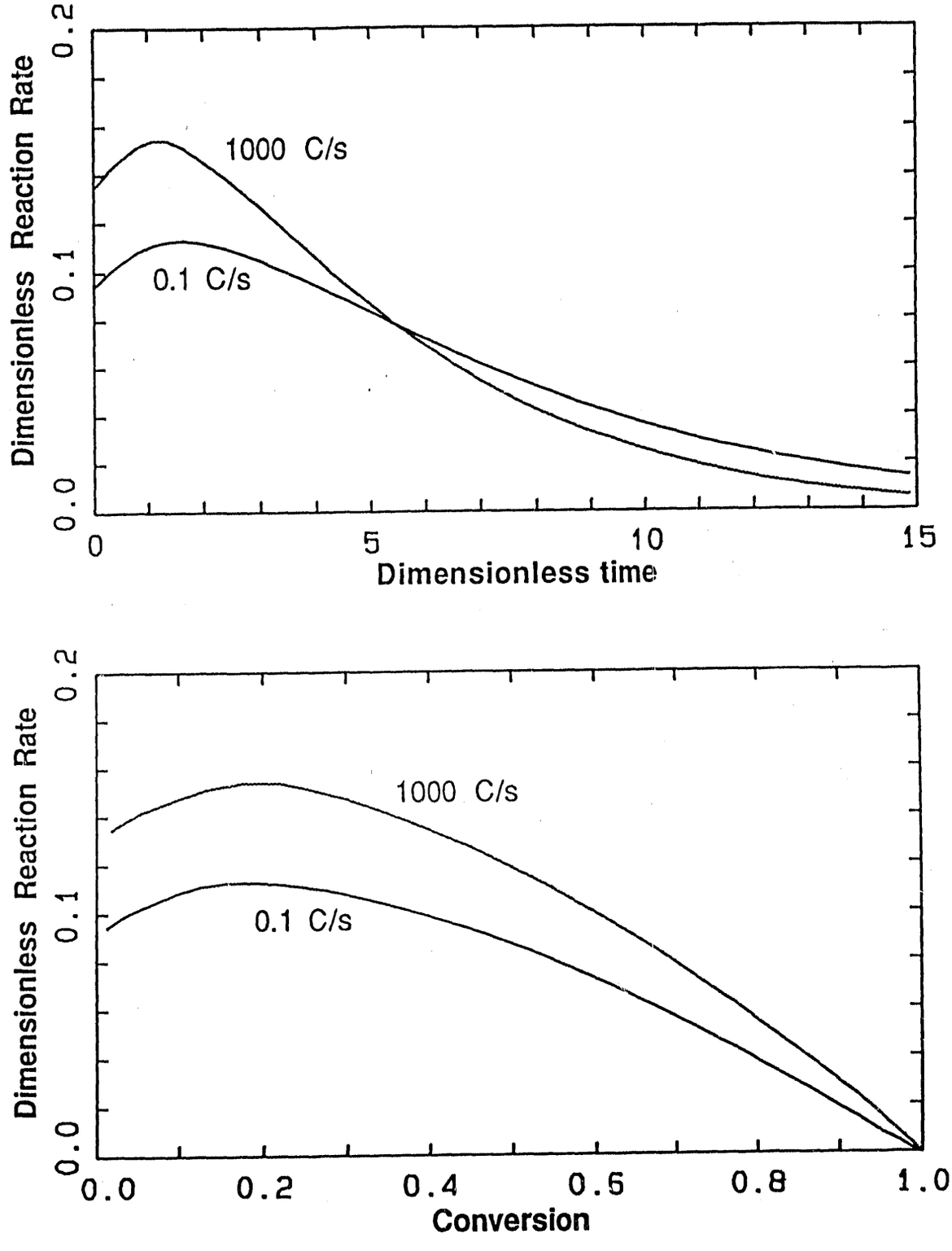

Figure 9: Reactivity patterns predicted for reaction in Regime A of two lignite chars produced at different pyrolysis heating rates (Coal particle size: 50-60 mesh). Each curve is the average computed from 48 runs with different particle cross-sections.

DATE
FILMED
07/8/92